Polysaccharides of Intracrystalline Glycoproteins Modulate Calcite Crystal Growth In Vitro

Shira Albeck, Steve Weiner, and Lia Addadi*

Abstract: Assemblies of glycoproteins from within the mineralized tissues of sea urchins and mollusks both interact in vitro in a similar manner with growing calcite crystals. A protein-rich fraction, a polysaccharide-rich fraction, and a fraction composed of densely glycosylated peptide cores were obtained by chemical and enzymatic treatment of the glycoproteins from sea-urchin spines. Each fraction was partially purified and characterized (amino acid composition, FTIR and NMR spectroscopy). A comparison of the interactions of these fractions with growing calcite crystals in vitro shows that the polysaccharide moieties of these glycoproteins are intimately involved in the interaction with growing calcite crystals on planes approximately parallel to the *c* crystallographic axis. Presumably the polysaccharides in the mollusk-shell glycoproteins are likewise responsible for the similar interactions of these macromolecules with calcite. We suggest that structured polysaccharide moieties of glycoproteins are important in controlling aspects of crystal growth in vivo as well.

Keywords
biomineralization · calcite · crystal morphology · glycoproteins · polysaccharides

Introduction

Organisms form their mineralized tissues in a wide variety of different ways and from different minerals. In some cases the mineral is amorphous, whereas in others it is crystalline. In the latter, the mineral may be deposited as large, unusually shaped single crystals, or as an array of usually smaller organized crystals, each with a well-defined shape. Thus, many organisms exert control over the mineral phase precipitated, the orientation of the crystals, as well as their shapes and textures.[1]

Dissolution of the externally cleaned crystal elements from various mineralized tissues releases into solution an ensemble of intracrystalline macromolecules.[2] These macromolecules clearly reside within the crystalline phase, where they create defects.[3] The distribution of these defects has been relatively well studied by X-ray diffraction, but much still remains to be learned about the macromolecules themselves. The distributions and compositions of these intracrystalline macromolecules vary between skeletal elements, suggesting that they may be employed by the organisms in a variety of ways, such as to control the morphology of the growing crystal and to improve its mechanical properties.

Information on possible modes of action of the intracrystalline macromolecules can be obtained by studying the interaction of solutions of the extracted macromolecules with growing calcite crystals in vitro. This interaction causes inhibition of crystal growth in the direction perpendicular to the plane of interaction, resulting in the expression of a new set of faces or the enhancement of existing ones. This in turn causes a macroscopic change in the morphology of the synthetic calcite crystal, which provides information on the molecular nature of the interaction.[4] Furthermore, by correlating the molecular motifs which characterize the affected crystal planes with the structures of the interacting moieties on the macromolecule, more insight can be obtained into the basic processes involved.

When macromolecules extracted from within the spines of the sea urchin (echinoderm) *Paracentrotus lividus* were introduced into solutions of growing calcite crystals, new faces other than the stable {104} faces were expressed.[5] These additional calcite planes are roughly parallel to the *c* crystallographic axis and correspond to the $\{\bar{1}0l\}$ sets of faces, with *l* ranging between 1 and 1.5.[6, 7, 8] A similar study of macromolecules extracted from within the calcitic prisms of the mollusk *Atrina rigida* showed that the quantitatively abundant proteins rich in aspartic acid interacted with planes perpendicular to the *c* crystallographic axis. In contrast, a minor fraction rich in glutamic acid and serine interacted with the same set of planes as did the sea-urchin macromolecules.[6] The latter observation was surprising, as the protein moieties are quite different in amino acid composition, yet the nature of the in vitro interactions appears to be the same.

The present work was therefore undertaken to investigate which moieties common to both the sea-urchin and the minor fraction of mollusk macromolecules are involved in the interaction with growing calcite crystals. The macromolecular assemblies were characterized by ^{1}H NMR and FTIR spectroscopy. This in turn required the development of a new decalcification method which does not utilize ethylenediaminetetraacetic acid (EDTA), as the presence of traces of EDTA in the preparation interferes with the interpretation of the spectroscopic data.

Here we show that both assemblies of macromolecules which interact with planes parallel to the *c* axis are glycosylated, while

[*] Prof. L. Addadi, S. Albeck, Prof. S. Weiner
Department of Structural Biology, Weizmann Institute of Science
Rehovot, 76100 (Israel)
Fax: Int. code +(8)344-136
e-mail: csaddadi@weizmann.weizmann.ac.il

0947-6539/96/0203-0278 $ 15.00+.25/0

those which interact with calcite planes perpendicular to the *c* axis are not. Furthermore, the protein-assembled polysaccharide moieties of the sea-urchin glycoproteins interact with distinct calcite planes which are almost parallel to the *c* axis, whereas the deglycosylated protein moieties of the same ensemble of macromolecules interact with planes oblique to the *c* axis. This detailed information on the various interacting moieties and their modes of interaction with synthetic calcite crystals contributes to our understanding of the mechanisms by which intracrystalline macromolecules regulate biological crystal growth.

Results

Dissolution of the Mineral Phase by an Ion-Exchange Resin: The first essential step in almost all studies of macromolecules from mineralized tissue is the dissolution of the mineral phase. Most studies use the calcium chelator EDTA at slightly basic pH or various types of acid. The former is very difficult to remove completely[9] and is usually very slow, and the latter denatures and possibly damages the proteins. Here, we employed a modification of a technique used to decalcify thin sections of bone for histology.[10] This method uses a cation-exchange resin that binds the calcium ions that are slowly released from the mineral into the undersaturated solution, and effectively removes them. By changing the solution daily, the pH is maintained between 4–5. This method is relatively rapid and does not introduce extraneous molecules which remain associated to the protein and which modify its properties. We were thus able to characterize the material extracted by this method spectroscopically, as well as analyze its interaction with growing calcite crystals in vitro.

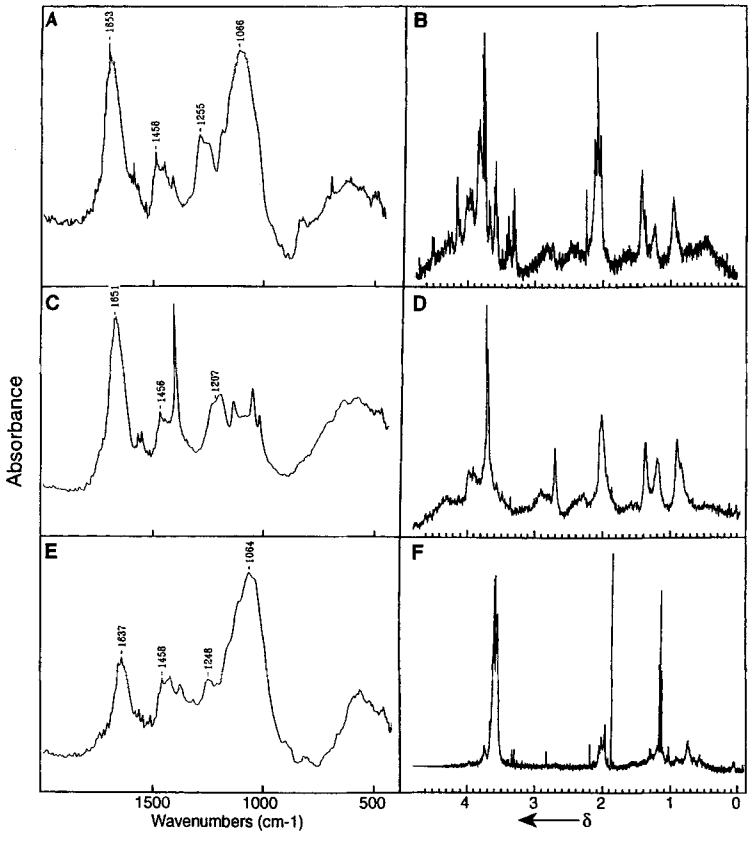

Fig. 1. Selected regions of IR and ^{1}H NMR spectra of glycoproteins extracted from within sea-urchin spines. A and B) IR and ^{1}H NMR spectra, respectively, of the untreated ensemble of glycoproteins. C and D) IR and ^{1}H NMR spectra, respectively, of polypeptides obtained by HF cleavage of saccharides from the glycoprotein ensemble. E and F) IR and ^{1}H NMR spectra, respectively, of glycopeptides obtained by treatment of the glycoproteins with proteases.

The total ensembles of macromolecules were extracted from within the mineral phase of the spines of the sea urchin *Paracentrotus lividus* and from within isolated prisms from the prismatic layer of the mollusk *Atrina rigida*. Amino acid analyses and ^{1}H NMR and FTIR spectroscopy were used to characterize the extracted soluble macromolecules from each of the mineralized tissues.

The Untreated Intracrystalline Macromolecules from the Spines of the Sea Urchin: There are two dominant features in the infrared spectrum of the ensemble of macromolecules from sea-urchin spines (Fig. 1 A): A protein amide I absorption band at 1653 cm^{-1} and the large absorption band occurring at around 1066 cm^{-1}. The latter suggests that these proteins are heavily glycosylated. The small peak at 1255 cm^{-1} may imply that some of the saccharide moieties are sulfated.[11]

Complementary results were obtained from the ^{1}H NMR spectrum of the same ensemble of macromolecules (Fig. 1 B). The relatively strong complex set of peaks in the region between $\delta = 3.3–3.9$ is caused by the overlap of most of the saccharide ring protons and some amino acid protons. The ^{1}H NMR spectrum provides a quantitative measure of the ratio between the saccharide and the protein in the glycoproteins. We took advantage of the fact that the resonance of each of the amino acid protons is well-known and that some of the peaks result from these resonances only (Table 2).[12] From this, and from the relative amount of the specific amino acid in the protein (known from amino acid analysis, Table 1), we calculated the average integrated area due to 1 mole of protons. Subtraction of the

Table 1. Amino-acid compositions and calculated saccharide/protein ratios for treated and untreated glycoproteins from the mineralized tissues of sea urchins and mollusks. The type of macromolecules obtained from the tissue and the procedure used in each case are shown in the head of the table.

	Sea-urchin spines			Mollusk prisms	
	Untreated	HF	Protease		Ion exchange
	Glyco-proteins	Proteins	Glycopeptides	Total protein ensemble	Minor fraction glycoproteins
Asx	12.5	12.7	12.1	54	12.0
Thr	6.3	8.4	12.7	1.9	9.3
Ser	3.8	3.4	5.6	3.3	7.1
Glx	8.3	14.4	5.9	20.7	21.2
Pro	13.0	14.0	9.3	1.6	6.1
Gly	17.8	17.5	13.5	3.4	5.7
Ala	10.8	11.0	11.4	8.2	14.0
Cys	0.2		0.5	0.4	2.5
Val	4.5	4.3	3.9	1.9	4.5
Met	4.4	3.0	12.7	0.3	0.8
Ile	3.7	2.1	3.0	0.5	2.8
Leu	4.3	2.8	2.2	1.0	4.0
Tyr	2.1	0.8	1.9	0.5	1.6
Phe	3.7	3.4	2.0	0.5	2.4
Lys	1.3	0.4	2.0	1.0	3.4
His	1.1	0.6		0.2	0.8
Arg	2.2	1.1	2.9	0.5	1.8
% aa [a]	100	>50	20	100	<10
r/100 aa [b]	38±14 (n = 6)	8±1 (n = 1)	67±13 (n = 1)	1±1 (n = 2)	29±4 (n = 2)

[a] % aa = Mole% amino acids of total extracted material. [b] *r*/100 aa = Calculated number of saccharide residues per 100 amino acids based on NMR data, presented as average ± estimated error; n = number of spectra.

  0947-6539/96/0203-0279 $ 15.00+.25/0

calculated contribution of amino acids from the integrated area of the peaks between $\delta = 3.3-3.9$ yielded the integrated area due to the resonance of the saccharide ring protons, which in turn allowed a rough evaluation of the number of saccharide residues per 100 amino acids (see Experimental Procedure). Intracrystalline macromolecules from the sea-urchin spines contained an average of 38 saccharide residues per 100 amino acids.

The extracted sea-urchin macromolecules were shown to interact with planes roughly parallel to the *c* crystallographic axis of calcite (Fig. 2A).[5] The fact that the sea-urchin macromolecules contain a significant amount of polysaccharide raised the possibility that the saccharide moieties may be involved directly in this mode of interaction. With this in mind, we investigated how the saccharide and protein moieties of the sea-urchin glycoproteins interact separately with calcite crystal planes. This involved three different preparation procedures: treatment of the glycoproteins with HF to remove the polysaccharide and to obtain the deglycosylated protein, treatment with an endoglycosidase to remove whole polysaccharide chains, and treatment with a mixture of proteases to yield densely glycosylated peptides. The resulting materials were characterized in terms of their amino acid contents, their saccharide/protein ratios based on ^{1}H NMR and FTIR, and the ways in which they interact with growing calcite crystals.

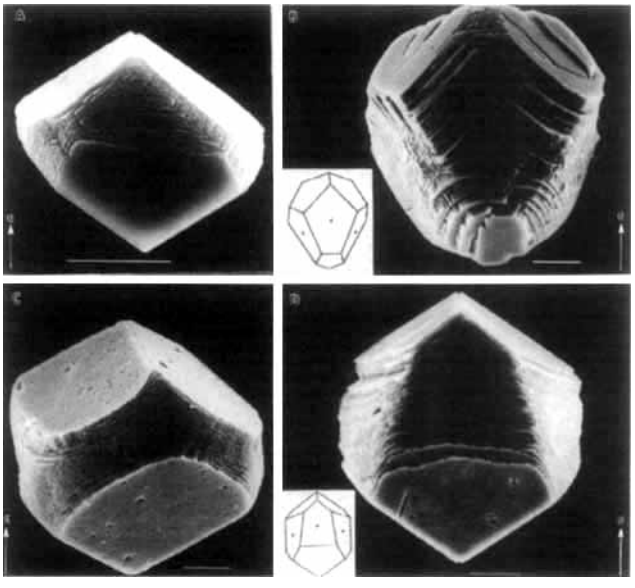

Fig. 2. Scanning electron micrographs of synthetic calcite crystals grown in the presence of fractions obtained by various treatments of glycoproteins extracted from sea-urchin spines. Note that the new faces induced by the additives express many steps, while the stable {104} faces are smooth. The scale bars represent 10 μm. A) Total untreated ensemble of glycoproteins (2 $\mu g\,mL^{-1}$). Note that the new faces produced are not well-defined. B) Polypeptides obtained by HF cleavage of saccharides from the glycoprotein ensemble. The new well-developed faces are oblique to the *c* crystallographic axis (in this crystal α is close to 21°, which corresponds to the {$\bar{2}$03} set of planes). Insert: computer simulation of the morphology of a crystal expressing the {$\bar{2}$03} faces (designated by circles). C) Pure polysaccharides removed from the glycoproteins by PNGase F. D) Glycopeptides obtained by treatment of the glycoprotein ensemble with proteases. The new well-developed faces are almost parallel to the *c* axis. In this crystal α is close to 5°, which corresponds to the {401} set of faces. Note that the inclination of the new planes relative to the *c* axis is in the opposite direction to those produced by the total untreated ensemble of glycoproteins and the deglycosylated proteins. Insert: computer simulation of the morphology of a crystal expressing the {401} faces (designated by circles).

Deglycosylated Protein: The sea urchin spine glycoproteins were subjected to HF cleavage followed by extensive dialysis. HF splits all O-glycosyl bonds gently to yield the corresponding monosaccharide fluorides, which spontaneously convert into the free monosaccharides after exposure to water.[13] N-Glycosyl bonds and peptide bonds are stable to HF under the conditions used. The HF-treated glycoproteins from the sea-urchin spines contained very little sugar, to judge by the IR spectrum (Fig. 1C). Analysis of the ^{1}H NMR spectrum (Fig. 1D) showed that at most 9 sugar residues per 100 amino acids remained attached to the protein. These saccharides may correspond to monosaccharides linked to Asn in cases where the polysaccharides are N-linked.

Calcite crystals grown in the presence of the deglycosylated protein at concentrations between 0.5–3 $\mu g\,mL^{-1}$ (amino acids, as determined by amino acid analysis) induced the formation of large well-developed rough faces inclined to the *c* crystallographic axis, in addition to the stable {104} faces. In several crystals an average inclination (α) of 21° was measured for the additional faces corresponding to the {$\bar{2}$03} set of crystallographic planes (Figs. 2B, 3). Note that large, well-defined faces are expressed at relatively low concentrations of protein compared with the untreated material.

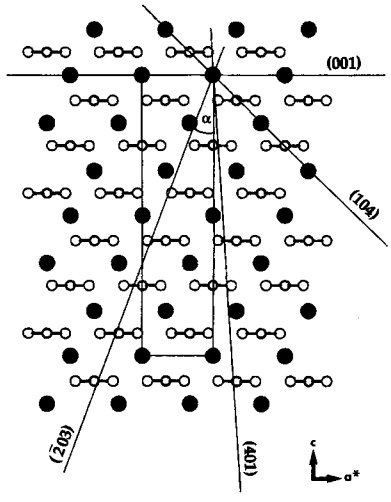

Fig. 3. Molecular structure of calcite viewed perpendicular to the *c* axis. The large atoms are calcium ions and the small atoms are the oxygen atoms of the carbonate molecules. α is the angle between the *c* axis and the newly developed face. The (104), (001), ($\bar{2}$03) and (401) faces are viewed edge-on.

Isolated Polysaccharides: PNGase F has a broad specificity, cleaving N-linked oligosaccharides at the N-glycosidic bond.[14] However, the polysaccharide moieties of the sea urchin spine glycoproteins were relatively resistant to treatment with this enzyme. They were, however, also resistant to base under reductive conditions. The latter treatment should remove saccharides which are O-linked to Ser or Thr.[15] Therefore, we attribute the relative lack of reactivity of the enzyme to steric hindrance, rather than to the dominance of O-linked saccharide moieties.

Partial purification of the PNGase F-treated material on a C18 Sep-Pak mini-column yielded a large fraction which contained a mixture of the unaffected glycoproteins and the partially deglycosylated glycoproteins, and a fraction which contained a small amount of pure polysaccharide. The pure polysaccharide was identified both by IR and ^{1}H NMR spectroscopy (not shown), and by the absence of protein in the amino acid analysis. When the polysaccharide was introduced into solutions of growing calcite, it interacted with a subset of all planes oriented approximately parallel to the *c* axis (Fig. 2C). This resulted in

0947-6539/96/0203-0280 $ 15.00+.25/0 Chem. Eur. J. 1996, 2, No. 3

the formation of crystals with rough curved surfaces, capped by rhombohedral faces. Note that a variety of monosaccharides at concentrations of up to 700 $\mu g mL^{-1}$ did not affect the crystallization of calcite, and produced perfect rhombohedral crystals.

Densely Glycosylated Peptides: Protease activity is restricted in the vicinity of densely glycosylated regions of the protein, presumably because of steric hindrance. Therefore, treatment of glycoproteins with a mixture of proteases is expected to hydrolyze the protein, but will still leave short peptides to which polysaccharides are attached. Sea-urchin glycoproteins treated with proteases followed by extensive dialysis lost 80% of their amino acids relative to the starting material. The IR spectrum of the product (Fig. 1 E) containing 20% of the amino acids showed a sharp increase in the proportion of polysaccharide, as judged by the enhancement of the peak around 1064 cm^{-1} relative to the amide I peak at 1637 cm^{-1}. The ^1H NMR spectrum of this product confirmed the loss of protein and the presence of a large saccharide component, with about 67 saccharide residues per 100 amino acids (Fig. 1 F). The amino acid composition of this mixture of glycopeptides (Table 1) exhibits several obvious differences compared with the composition of the starting material. The decrease in the proportion of Glx, the increase in the proportion of Thr, and the 1:1 ratio of the amount of Asx and Thr suggest the presence of N-linked sugars, in the typical sequence Asn-X-Thr. Note that in the amino acid analysis the large increase in the region where Met elutes is probably caused by amino sugars.

Calcite crystals grown in the presence of the glycopeptides thus obtained at concentrations between 0.1–2.0 $\mu g mL^{-1}$ (amino acids, determined by amino acid analysis) expressed well-developed faces other than the stable {104} faces. The new rough faces are very close to {010}. The slight inclination (around 5°) of the new faces with respect to the *c* axis is in the opposite direction to that produced by the ensemble of glycoproteins (Fig. 2D, 3). At a concentration of over 2 $\mu g mL^{-1}$ (amino acids) inhibition of calcite crystallization occurred. Note that the effective concentration of the glycopeptide is significantly smaller than that of the ensemble of glycoproteins.

Intracrystalline Macromolecules from the Mollusk Prisms: The infrared spectrum of the *Atrina* ensemble of macromolecules (Fig. 4A) has a protein amide I absorption at 1653 cm^{-1}, as well as relatively strong carboxylate absorption bands at around 1575 and 1417 cm^{-1}. The latter absorption bands are consistent with the high Asp and Glu content of the intraprismatic proteins (Table 1). The infrared absorption bands associated with polysaccharide at around 1050 cm^{-1} are very small in this ensemble of macromolecules. Furthermore, the typical peaks associated with saccharides in the region between $\delta = 3.3-3.9$ are almost absent in the ^1H NMR spectrum (Fig. 4B); this reinforces the notion that these macromolecules contain very little saccharide, if any at all.

While the quantitatively major acidic fraction of this ensemble was shown to interact with planes perpendicular to the *c* crystallographic axis of calcite, a minor fraction interacted in a way similar to the sea-urchin ensemble of glycoproteins, producing new calcite faces roughly parallel to the *c* crystallographic axis.[6] The large infrared absorption band at around 1057 cm^{-1} (Fig. 4C) and the relatively large peaks in the region between $\delta = 3.3-3.9$ of the ^1H NMR spectrum (Fig. 4D) suggest that the minor fraction is glycosylated (with an average of 29 saccharide residues per 100 amino acids). In contrast, the infrared spectrum of the major acidic fraction is almost identical to that of the total ensemble and contains little or no polysaccharide as inferred from the absence of peaks around 1050 cm^{-1} (data not shown). Thus, the interaction with planes parallel to the *c* axis of calcite involves the participation of glycoproteins, while the interaction with planes perpendicular to the *c* axis involves non-glycosylated proteins.

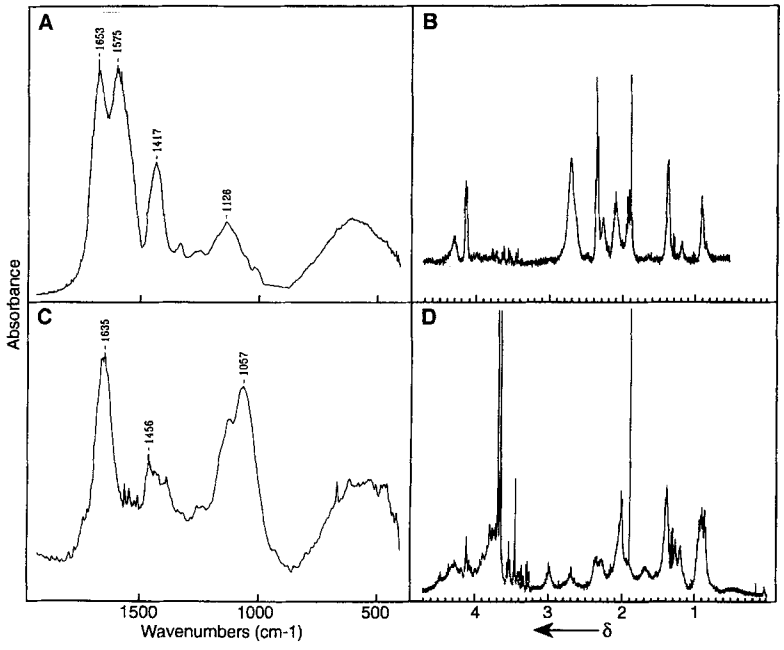

Fig. 4. Selected regions of IR and ^1H NMR spectra of macromolecules extracted from within prisms of *Atrina*. A and B) IR and ^1H NMR spectra, respectively, of the total ensemble of macromolecules. C and D) IR and ^1H NMR spectra, respectively, of the minor fraction of macromolecules containing glycoproteins, obtained by anion exchange separation of the total ensemble of macromolecules.

Discussion

We have shown that certain matrix glycoproteins from calcitic skeletal elements of mollusks and echinoderms interact in a similar manner with growing calcite crystals in vitro. The polysaccharide moieties of these macromolecules are intimately involved in these interactions, provided that they are still linked to a polypeptide core. We elucidated aspects of these interactions by investigating separately a polysaccharide fraction, densely glycosylated peptide cores, and a protein-rich fraction, and comparing these results with the interactions of the intact macromolecules.

Small amounts of pure polysaccharides, removed enzymatically from the sea urchin spine glycoproteins, interacted with growing calcite in a nonspecific manner. They induced the formation of a subset of many faces oriented approximately parallel to the *c* axis. This type of interaction endows the crystal with a round and smooth appearance on surfaces parallel to the *c* axis. In contrast to the flat surfaces of inorganic calcite crystals, the sea-urchin skeletal calcite crystals are also smooth and rounded. It is conceivable that this type of nonspecific interaction of the polysaccharides is directly relevant to the formation of the smooth and rounded morphologies in vivo. We caution, however, that many polymeric and monomeric additives inter-

act in vitro in such a way with calcite crystals. Only the development of a defined set of faces in the presence of an additive is indicative of a specific interaction between the two and can be regarded as being characteristic of controlled processes.[16]

It is not surprising that the free polysaccharides do not interact with a defined set of planes, since in the course of their release into solution these polymers probably lose any ordered conformation required for a cooperative interaction with a specific crystal plane. Unlike proteins and polynucleic acids, polysaccharides form very weak intramolecular interactions, which are required for the formation of ordered structures. Conformational stability can, however, occur when a large number of polysaccharides acts cooperatively, usually by intermolecular interactions between two or more aligned chain segments.[17] This can be achieved in part by the adjacent attachment of several polysaccharide chains to a protein core.

Densely glycosylated peptide cores were produced by protease treatment of the glycoproteins. These cores did interact with well-defined crystal planes, producing faces which are very close to {010}. We suggest that the densely glycosylated regions of the peptide form assemblies of ordered structure that are capable of interacting with distinct crystal planes. This is consistent with the observations that polysaccharides extracted from within the coccoliths of *E. huxleyi* interacted in a nonspecific manner producing many faces roughly parallel to the *c* axis of calcite, while alginic acid interacted with distinct planes which were very close to {010}.[18] Unlike the coccolith polysaccharide, alginic acid forms dimers by alignment of two polymers in the presence of calcium. These in turn endow the polysaccharide with a regular secondary conformation.[17]

Treatment of the glycoproteins with HF produced a protein-rich fraction with only small amounts of Asn-linked monosaccharides. This protein moiety interacted very strongly with one set of calcite planes that is oblique to the *c* axis. While the purified protein moieties and the densely glycosylated peptide cores interact from solution with well-defined crystal planes, the intact glycoproteins do not. Instead they induce the formation of several closely related faces oblique and parallel to the *c* axis. Hence, the polysaccharide moieties on the protein contribute a spectrum of interactions which are not observed upon removal of most of the polysaccharide from the glycoproteins by HF. In vivo, the glycoproteins are located within the calcite crystals and are intimately associated with the mineral phase. Upon dissolution of the mineral, the released glycoproteins are probably partially denatured, exposing some moieties and concealing others in a non-native conformation. Consequently, exposed protein regions and assembled polysaccharide moieties may react simultaneously in an independent manner producing the combination of effects which we observe in vitro. It is interesting to note that calcite crystals grown epitaxially on the surfaces of sea-urchin skeletal elements develop the same faces as the glycoproteins.[8] Under these conditions the glycoproteins released from the surfaces of the biogenic element by mild etching undergo minimal structural modification prior to being readsorbed on the newly crystallizing calcite. Thus the intact glycoproteins interact with calcite crystals in a manner similar to those in close-to-native conformation. We cannot rule out the possibility that some of these glycoproteins are partially associated with other macromolecules, surfaces or membranes in vivo. Therefore, our in vitro assay can identify interactions which may take place in vivo, but is unable to mimic the manner in which the organism coordinates the separate interactions to achieve the desired control of crystal growth.

Polysaccharides, and in particular sulfated mucopolysaccharides, are known to be closely associated with mineralization in vertebrates[19] and invertebrates.[20] Some studies clearly show their involvement in the nucleation process.[21] Among the best-characterized polysaccharide-containing macromolecules associated with mineralization are two of the many proteins in bone, bone sialoprotein and osteopontin.[22] In many mineralized tissues, a distinction is now made between matrix macromolecules located outside crystals (intercrystalline) and those located within crystals (intracrystalline). The former may also contain structural polysaccharides such as chitin[23] as well as glycoproteins. Glycoproteins have also been identified in the intracrystalline macromolecules of sea-urchin larvae,[2a] brachiopods,[2b] and Coccolithophoridae.[2c]

The possible roles of glycoproteins in mineral formation have been investigated by several groups. Kinetic studies showed inhibition of calcium carbonate precipitation in the presence of some glycoproteins in vitro.[24] Tunicamycin, an inhibitor of the formation of N-linkage of glycoproteins, inhibited gastrulation and spicule formation by sea-urchin embryos.[25] A monoclonal antibody directed against a carbohydrate epitope of a glycoprotein isolated from sea-urchin larvae inhibited calcium uptake and spicule formation in vitro.[26] Very little was known, however, about the direct involvement of the glycoproteins with the mineral or the role played by the carbohydrate side chains in the mode of action of glycoproteins.

The two classes of matrix macromolecules present in the mineralized tissues studied here, the Asp-rich proteins and the glycoproteins, may perform different functions in crystal formation in vivo. The Asp-rich proteins are capable in vitro of actively inducing, regulating, and inhibiting crystal growth along the *c* crystallographic axis by interacting with {001} planes.[27] The glycoproteins investigated, on the other hand, inhibit crystal growth in the direction perpendicular to the *c* axis. Hence, one possible function of the glycoproteins could be a stereochemical modulation of biological crystal morphology. Another demonstrated function of the sea-urchin glycoproteins is modification of the fracture properties of the calcite crystals. Inorganic calcite is very brittle and cleaves easily along {104} planes. Synthetic calcite crystals with occluded sea-urchin glycoproteins fracture with a conchoidal cleavage reminiscent of amorphous materials. We have speculated that this is because of the deviation of crack propagation caused by glycoproteins located on crystal planes that are oblique to the {104} cleavage planes.[5, 28]

Too little is known, as yet, about the composition and structures of these polysaccharides even to speculate about the nature of their molecular interactions with calcite planes. Our results do, however, indicate that the interactions of glycoproteins with planes parallel to the *c* axis involve both rigid structural and stereochemical requirements, which are hard to mimic in our in vitro experiment. The organisms, on the other hand, can control the time, place, concentration and sequence in which macromolecules are secreted into the mineralization site. It is most likely that they also take advantage of the fact that polysaccharides can form a variety of subtly different structures that could be used for "fine-tuning" the interactions.

Concluding Remarks

Until now many studies of matrix macromolecular functions have focused on the protein moieties. Schemes have been presented which envisage protein surfaces with ordered arrays of charged amino acids that interact specifically with regularly structured crystal surfaces.[1, 29] The association of considerable numbers of polysaccharide chains with the protein backbone,

0947-6539/96/0203-0282 $ 15.00+.25/0 Chem. Eur. J. 1996, 2, No. 3

however, can endow the polypeptide portion with a high degree of chemical and physical diversity. Here we have shown that the polysaccharide moieties of these glycoproteins are also involved in certain types of interactions with calcite crystals. Much still remains to be understood, however, about the structural and stereochemical nature of these polysaccharide–crystal interactions.

Experimental Procedure

Skeletal Element Preparation: Adult specimens of the echinoid *Paracentrotus lividus* were collected alive from Atlit, Israel. The spines were removed and treated with 2.5% NaOCl solution overnight on a rocking table to remove extraskeletal organic residues. They were then extensively washed with double distilled water (DDW) and stored dry at room temperature. Shells of the bivalve mollusk *Atrina rigida* were collected alive off the coast of North Carolina, USA. The soft parts were removed and the shells stored dry. The calcitic prismatic layer was mechanically separated from the inner nacreous layer and treated with 12% NaOCl solution while stirred constantly for 4 days, with two changes of the solution. The crystal suspension was sonicated for 10 min and allowed to settle (15 min), and the NaOCl was then removed by decantation. The disaggregated crystals were washed with 10 changes of DDW. The crystalline skeletal elements were examined in a Jeol 6400 scanning electron microscope (SEM) to verify surface cleanliness and, in the case of the mollusk shells, to verify that the single-crystalline elements were completely disaggregated.

Decalcification by Ion Exchange Resin: The clean, dry single crystals were ground in a mortar. The fine powder was suspended in DDW (50 mL per 2 g mineral) and poured into a dialysis tube (Spectrapor 3 tubing with a molecular weight cutoff of 3500 daltons, diameter 34 mm). The dialysis bag was placed in a glass tube (30 × 6 cm) and the two ends of the bag fastened to the rubber stoppers at the ends of the tube. Dowex 50 × 8 cation-exchange resin (Sigma, H^+ form, mesh 50–100; 100 g) prewashed with DDW was placed in the glass tube and DDW was added to fill it. The tube was continuously rotated (16 rpm) in a propeller-like mode at room temperature to keep the resin and mineral in suspension. The DDW was changed daily and the gas which accumulated inside the dialysis bag removed. The decalcification of 2 g of mineral takes 2–5 days. After complete decalcification, the contents of the dialysis bag were extensively dialyzed against DDW and the soluble and insoluble materials were separated by centrifugation at 3000 g for 10 min. The soluble material was lyophilized and stored at −22 °C for further analysis.

Amino Acid Analysis: Aliquots of the protein solution were lyophilized and hydrolyzed under vacuum in 6 N HCl (0.3 mL) at 112° for 24 h after flushing twice with nitrogen. Following evaporation of the HCl, the hydrolysates were analyzed on a Dionex BIOLC amino acid analyzer with ninhydrin detection.

Crystal Growth Experiments: Synthetic calcite crystals were grown in Nunc multidishes with well diameters of 1.5 cm in which clean glass coverslips of 1.3 cm diameter (Fisons) were placed. A total volume of 0.75 mL of 10 mM calcium chloride solution was introduced into each well, the wells were covered with aluminum foil and punctured by a needle. Calcite crystals were grown for 2 days by slow diffusion of ammonium carbonate in a closed desiccator [4c]. When the effect of additives was studied, aliquots of concentrated solutions of the additive were added to the above calcium chloride solution. Each crystallization experiment included controls of pure calcium chloride solution. The crystals grown in the absence of additives always had perfect rhombohedral morphology.

The glass coverslips covered with calcite crystals were lightly rinsed with DDW, dried, and glued to SEM stubs. After gold coating, the crystals were observed in the SEM. In order to identify the new $\{h0l\}$ faces [7], the crystals were viewed with their $\{h0l\}$ and corresponding $\{104\}$ faces both edge-on. In this position the c crystallographic axis lies in the plane of the picture, allowing the measurement of the α angle, which is the angle between the c axis and the unknown $\{h0l\}$ face. This angle unequivocally identifies the Miller indices of the face [8]. The sign of h and l is defined by the angle between the new face and the $\{104\}$ face both in the edge-on position (Fig. 3). When h and l are of the same sign, the new face forms an angle of $(135 + \alpha)°$ with the (104) face, while a face for which h and l have opposite signs will form an angle of $(135 - \alpha)°$. Calcite crystals grown in the presence of the deglycosylated proteins expressed faces which formed an angle of less than 135° between the new face and $\{104\}$ face in the edge-on position corresponding to $\{\bar{h}0l\}$ faces. In contrast, calcite grown in the presence of the glycopeptides expressed faces which formed an angle of over 135° in the same position corresponding to $\{h0l\}$ faces.

FTIR Spectrometry: A few tens of micrograms of dry sample were uniformly ground in an agate mortar. The sample was mixed with about 70 mg of KBr (IR grade). A 7-mm pellet was made without evacuation. The spectra were recorded (4 cm^{-1} resolution) with a computer-controlled spectrometer (MIDAC, Costa Mesa, CA, USA). The spectrum of pure KBr was subtracted from the spectrum of the sample in KBr. The band occurring at 1660–1630 cm^{-1} is assigned to the amide I vibrational modes of the protein, and possibly to the N-acetyl groups of polysaccharide. The band at 1575 cm^{-1} could be caused by the amide II absorption, but this has been observed to be weak in mollusk shell proteins [9b]. We suspect that it is due to absorption by the calcium-loaded carboxylate groups. IR bands around 1600 and 1400 cm^{-1} are assigned to the carboxylate groups. The absorption bands in the 1400–1200 cm^{-1} region can be assigned primarily to coupled vibrations of the C-C-H, O-C-H, and C-O-H groups. Bands occurring around 1255 and 1230 cm^{-1} are tentatively assigned to sulfate-related modes and/or the amide III absorption [11]. The region of the IR spectrum from 1200–1000 cm^{-1} is associated mainly with C-C-O and C-O-C stretchings of the pyranose ring structures of saccharides [30].

^{1}H NMR Spectroscopy: Dry samples were dissolved in D_2O (Merck) in a concentration of at least 5 μmole amino acids per 500 μL. Spectra were run on a Bruker AMX400 spectrometer with the water peak at $\delta = 4.8$ as reference. Typically between 500–1000 scans were collected at room temperature. Suppression of the water peak often resulted in the reduction or disappearance of some of the peaks corresponding to the anomeric protons of the sugar and α-H of protein, which resonate in this region. Regions where different amino acid protons are expected to resonate have been assigned (Table 2) [12]. The characteristic features of the

Table 2. Measured integrated areas of NMR peaks and their assignment to resonating protons of treated and untreated macromolecules from sea-urchin and mollusk skeletal elements.

		Integrated area of NMR peaks				
		Sea-urchin spines			Mollusk prisms	
δ	Resonating Protons	Untreated	HF-Treated	Protease-Treated	Minor fraction	Total ensemble
0.8–1.0	γ-CH_3(Val), γ-CH_3 (Ile), δ-CH_3 (Ile), δ-CH_3 (Leu)	0.85	1.39	4.28	4.23	1.83
1.0–1.5	γ-CH_3 (Thr), γ-CH_2 (Lys), β-CH_3 (Ala), γ-CH_2 (Ile)	1.26	1.62		4.46	2.60
1.5–1.8	β-CH_2 (Leu), δ-CH_2 (Lys) γ-CH_2 (Arg), γ-CH (Leu)	0.35			1.42	
1.8–2.4	β-CH (Ile), β-CH_2 (Lys), β-CH_2 (Arg), β-CH (Val), β,γ-CH_2 (Pro), β,γ-CH_2 (Glx), β-CH_2 (Met), ε-CH_3 (Met), CH_3-NAc	2.72	3.61	6.13	7.33	8.38
2.4–2.8	β-CH_2 (Asx), γ-CH_2 (Met)	0.56	1.27 [a]		1.29	5.29
2.8–3.3	ε-CH_2 (Lys), β-CH_2 (Phe), β-CH_2 (Tyr), δ-CH_2 (Arg)				1.00	
3.3–3.9	δ-CH_2 (Pro), β-CH_2 (Ser), saccharide ring protons	4.34 [b]	2.20	27.41	11.30 [b]	1.31
3.9–4.0	α-H (Gly), α-H (Val)		1.00			

[a] Integrated area measured in the range $\delta = 2.4–3.3$. [b] Integrated area measured in the range $\delta = 3.3–4.0$.

^{1}H NMR spectra of polysaccharides are the overlap of most of the saccharide ring protons in the region $\delta = 3.3–3.9$, the methyl protons of N-acetyl group between $\delta = 1.9–2.1$, and the occurrence of some well-resolved resonances associated with the anomeric protons between $\delta = 4.0–5.2$ [31]. Calculation of the average integrated area due to 1 mole of protons was carried out by dividing the measured integrated area of a given peak (Table 2) by the relative number of moles of amino acids (Table 1) and by the number of resonating protons contributing to that peak. Subtraction of the calculated weighted integration due to the δ-CH_2 of Pro and β-CH_2 of Ser from the measured integrated area between $\delta = 3.3–3.9$ yielded the area associated with the resonance of saccharide protons only. This value divided by the average integrated area of 1 mole of protons and by six (the number of ring protons) yielded the number of saccharide residues per 100 amino acids. Owing to the broad and often convoluted peaks from resonating protons in mixtures of macromolecules, it is very difficult to assign the peaks to specific protons. Furthermore, it is often difficult to obtain integrated areas of single peaks. Therefore, we have used groups of peaks both in the assignment to the resonating protons and in the measurement of the integrated area (Table 2). Consequently, this calculation yields only a rough estimate of the number of saccharide residues.

Protease Digestion: Glycoprotein (5 μmole, determined by amino acid analysis) was dissolved in sodium phosphate buffer (100 mM, pH 7.8, 1 mL). Pronase (protease type XIV from *Streptomyces griseus*, Sigma; 10 μg) was added and the solution was left for 18 h at 37 °C. Protease from *Staphylococcus aureus* V 8 (Sigma; 50 μg) and trypsin (Sigma; 10 μg) were added and left for an additional 12 h at 37 °C. Following centrifugation, the solution was extensively dialyzed against DDW.

PNGase F Treatment: Sea-urchin glycoprotein (9 μmole) was dissolved in denaturing buffer (700 μL) containing 0.5% SDS and 1% mercaptoethanol by heating at 100 °C for 2 min. Reaction buffer was added to make a 0.05 M sodium phosphate solution (pH 7.5). 1% NP-40 followed by 20 units of PNGase F (New England Biolabs) were added and incubated for 12 h at 37 °C. An additional 20 units were added the next day and left for another 12 h under the same conditions. The product was dialyzed and separated by reverse phase chromatography on a Sep-Pak C18 cartridge (Waters Associates) [2d]. The mixture was dissolved in sodium acetate (5.0 mL, 0.05 M, pH 6.5) and then passed through the cartridge 5 times by means of a syringe. The cartridge was then flushed 5 times with 5.0 mL of 50% acetonitrile in sodium acetate (0.05 M, pH 6.5). Finally the cartridge was flushed with 5.0 mL of dimethylsulfoxide. The three fractions were dialyzed separately against DDW, lyophilized and analyzed by FTIR, NMR and amino acid analysis. The first wash contained the glycoprotein, partially deglycosylated glycoprotein and the enzyme, while the second and the last washes contained small amounts of polysaccharide that had been removed.

HF Treatment: Glycoproteins (5 μmole) were lyophilized in a Teflon tube. HF (3 mL) was allowed to condense in the tube, which was immersed in an ice bath under nitrogen. The solution was stirred for 3 h at 0 °C. Evaporation of HF was carried out under vacuum followed by extensive dialysis against DDW.

Acknowledgments: We thank Joanna Aizenberg for her help in the determination of the crystallographic planes and for her valuable advice. We also thank Dr. Yechiel Shai for his assistance with the HF cleavage, Dr. Elisha Berman, Hebrew University, for his helpful discussion on NMR of glycoproteins, and Mircha Greenberg for the measurement of the ^{1}H NMR spectra. S. W. is incumbent of the I. W. Abel Professorial Chair of Structural Biology, and L. A. is incumbent of the Patrick E. Gorman Professorial Chair of Biological Ultrastructure. This study was funded by grant no. 92-00100 from the US-Israel Binational Science Foundation.

Received: August 4, 1995 [F183]

[1] a) H. A. Lowenstam, S. Weiner, *On Biomineralization*, Oxford University Press, NY, **1989**; b) K. Simkiss, K. M. Wilbur, *Biomineralization. Cell Biology and Mineral Deposition*, Academic Press, San Diego, **1989**.

[2] a) S. C. Benson, N. C. Benson, F. Wilt, *J. Cell Biol.* **1986**, *102*, 1878–1886; b) M. J. Collins, G. Muyzer, G. B. Curry, P. Sandberg, P. Westbroek, *Lethaia* **1991**, *24*, 398; c) E. W. de Jong, L. Bosch, P. Westbroek, *Eur. J. Biochem.* **1976**, *70*, 611–621; d) S. Weiner, *J. Exp. Zool.* **1985**, *234*, 7–15.

[3] a) A. Berman, J. Hanson, L. Leiserowitz, T. F. Koetzle, S. Weiner, L. Addadi, *Science* **1993**, *259*, 776–779; b) A. Berman, J. Hanson, L. Leiserowitz, T. F. Koetzle, S. Weiner, L. Addadi, *J. Phys. Chem.* **1993**, *97*, 5162–5170.

[4] a) L. Addadi, Z. Berkovitch-Yellin, N. Domb, E. Gati, M. Lahav, L. Leiserowitz, *Nature* **1982**, *296*, 21–26; b) Z. Berkovitch-Yellin, J. van Mil, L. Addadi, M. Idelson, M. Lahav, L. Leiserowitz, *J. Am. Chem. Soc.* **1985**, *107*, 3111–3122; c) L. Addadi, S. Weiner, *Proc. Natl. Acad. Sci. U. S. A.* **1985**, *82*, 4110–4114.

[5] A. Berman, L. Addadi, S. Weiner, *Nature* **1988**, *331*, 547–548.

[6] S. Albeck, J. Aizenberg, L. Addadi, S. Weiner, *J. Am. Chem. Soc.* **1993**, *115*, 11691–11697.

[7] Crystal faces are denoted by a set of Miller indices *h*, *k*, *l*, that define their orientation relative to the crystal axes. {*h*,*k*,*l*} denotes the family of symmetry-related faces (*h*,*k*,*l*). In hexagonal space groups, the symmetry-related {*hkl*} planes are (*hkl*), (*k*, −(*h* + *k*),*l*), (−(*h* + *k*),*h*,*l*) and their Friedel pairs. For example, for the {104} family the symmetry-related planes are (104), (01$\bar{4}$), ($\bar{1}$14), ($\bar{1}$0$\bar{4}$), (01$\bar{4}$) and (1$\bar{1}\bar{4}$).

[8] J. Aizenberg, S. Albeck, S. Weiner, L. Addadi, *J. Crystal Growth* **1994**, *142*, 156–164.

[9] a) A. P. Wheeler, K. W. Rusenko, J. W. George, C. S. Sikes, *Comp. Biochem. Physiol.* **1987**, *87B*, 953–960; b) D. Worms, S. Weiner, *J. Exp. Zool.* **1986**, *237*, 11–20.

[10] L. B. Dotti, G. P. Paparo, B. E. Clarke, *Am. J. Clin. Pathol.* **1951**, *21*, 475.

[11] a) J. J. Cael, D. H. Isaac, J. Blackwell, J. L. Koenig, *Carbohydr. Res.* **1976**, *50*, 169–179; b) F. Cabassi, B. Casu, A. S. Perlin, *Carbohydr. Res.* **1978**, *63*, 1–11.

[12] A. Bundi, K. Wüthrich, *Biopolymers* **1979**, *18*, 285–298.

[13] J. Lechner, F. Wieland in *Methods in Molecular Biology, Vol. 14* (Ed.: E. F. Hounsell), Humana, Totowa, **1993**.

[14] F. Maley, R. B. Trimble, A. L. Tarentino, T. H. Plummer, Jr., *Anal. Biochem.* **1989**, *180*, 195–204.

[15] D. M. Carlson, *J. Biol. Chem.* **1968**, *243*, 616–626.

[16] L. Addadi, J. Moradian-Oldak, S. Weiner in *Surface Reactive Peptides and Polymers* (Eds.: C. S. Sikes, A. P. Wheeler), *ACS Symp. Ser.* **1991**, pp. 13–27.

[17] D. A. Rees, E. J. Welsh, *Angew. Chem.* **1977**, *89*, 228–239; *Angew. Chem. Int. Ed. Engl.* **1977**, *16*, 214–224.

[18] J. M. Didymus, P. Oliver, S. Mann, A. L. DeVries, P. V. Hauschka, P. Westbroek, *J. Chem. Soc. Faraday Trans.* **1993**, *89*, 2891–2900.

[19] W. D. Armstrong, *Symposium on Phosphorus Metabolism, Vol. 2*, **1952**, p. 698.

[20] A. Abolins-Krogis, *Acta Zoologica* **1958**, *39*, 1–20.

[21] a) M. A. Crenshaw, H. Ristedt, *Biomineralization* **1975**, *8*, 1–8; b) K. Wada, *Bull. Natl. Pearl Res. Lab.* **1961**, *7*, 703; c) K. Wada in *The Mechanisms of Biomineralization in Animals and Plants* (Eds.: M. Omori, N. Watabe), Tokai University Press, Tokyo, **1980**, pp. 79–92.

[22] a) J. Chen, M. D. McKee, A. Nanci, J. Sodek, *Histochem. J.* **1994**, *26*, 67–78; b) R. T. Ingram, B. L. Clarke, L. W. Fisher, L. A. Fitzpatrick, *J. Bone Miner. Res.* **1993**, *9*, 1019–1029.

[23] C. Jeunieux in *Comprehensive Biochemistry, Vol. 26* (Eds.: M. Florkin, E. H. Stotz), Elsevier, Amsterdam, **1971**, pp. 595–632.

[24] a) A. P. Wheeler, J. W. George, C. A. Evans, *Science* **1981**, *212*, 1397–1398; b) A. H. Borman, E. W. de Jong, M. Huizinga, D. J. Kok, P. Westbroek, L. Bosch, *Eur. J. Biochem.* **1982**, *129*, 179.

[25] E. G. Schneider, H. T. Nguyen, W. J. Lennarz, *J. Biol. Chem.* **1978**, *253*, 2348–2355.

[26] M. C. Farach-Carson, D. D. Carson, J. L. Collier, W. J. Lennarz, H. R. Park, G. C. Wright, *J. Cell Biol.* **1989**, *109*, 1289–1299.

[27] a) L. Addadi, S. Weiner, *Proc. Natl. Acad. Sci USA* **1985**, *82*, 4110–4114; b) L. Addadi, S. Weiner, *Mol. Cryst. Liq. Cryst.* **1986**, *134*, 305–322.

[28] L. Addadi, S. Weiner, *Angew. Chem.* **1992**, *104*, 159–176; *Angew. Chem. Int. Ed. Engl.* **1992**, *31*, 153–169.

[29] *Biomineralization. Chemical and Biochemical Perspectives* (Eds.: S. Mann, J. Webb, R. J. P Williams), VCH, Weinheim, **1989**.

[30] F. S. Parker in *Application of Infrared Spectroscopy in Biochemistry, Biology and Medicine*, Plenum, NY, **1971**, p. 601.

[31] J. F. G. Vliegenthart, L. Dorland, H. van Halbeek in *Advances in Carbohydrate Chemistry and Biochemistry, Vol. 41* (Eds.: R. S. Tipson, D. Horton), Academic Press, NY, **1983**, pp. 209–374.

0947-6539/96/0203-0284 $ 15.00+.25/0